It is highly important to estimate an evolution of the jet's radius to get support of the assumptions made or obtain an idea on how to correct solution in a good correspondence to the existing experimental data. For this the Bernoulli equation and the mass conservation equation are considered for the jet penetrating a pool as follows:

$$S_1((\rho_1-\rho_2)hg+0.5\rho_1 v_1^2)=0.5\rho_1 u_0^2 S_0\ ,$$
$$\rho_1 v_1 S_1=\rho_1 u_0 S_0\ . \tag{8}$$

Here S is the cross section area of the jet. Indexes 0 and 1 denote the initial state and the current state of the jet.

3.2 Dimensionless conservation equations for the jet

In a dimensionless form, retaining the same symbols, the equation array (8) yields:

$$S_1\left[2h(1-\rho_{21})/Fr+v_1^2\right]=1,$$
$$S_1 v_1=1. \tag{9}$$

The equation array (9) has the following solution:

$$S_1=\frac{Fr}{4h(1-\rho_{21})}\left[1\pm\sqrt{1-8h(1-\rho_{21})/Fr}\right],$$
$$v_1=1/S_1 \tag{10}$$

As follows from (10), both possible values of the jet radius are available. One is the initial jet radius while the other value means that jet may loose its stability and change the radius abruptly as we could see from the experimental data above.

3.3 Bifurcation of a jet

Thus, we have got quite unexpected result (10), where from follows that there are two available solutions for the jet radius, with the point of bifurcation, which depends on the Fourier number and density ratio as follows:

$$h=\frac{Fr}{8(1-\rho_{21})}. \tag{11}$$

After the point of bifurcation (11) the solution (10) does not exist in real numbers, therefore the jet can switch its radius abruptly between two available stable states.

The jet starts penetration into the pool with initial cross-sections, thus, S_1=1. Further analysis of the equation (11) shows that for a small penetration depth or, more generally, in case of

$$8h(1-\rho_{2/1})<<Fr\,, \tag{12}$$

Solution (10) gives the following pair of the available jet radiuses to switch between them:

$$S_1\approx 1,$$
$$S_1\approx\frac{Fr}{2h(1-\rho_{21})}>>1. \tag{13}$$

3.4 Specific features of the jet penetration

Thus, there is no reason for a jet to become abruptly from the section area 1 to the bigger one at the beginning of its penetration into a pool of other liquid because the jet momentum directs mainly along its axis. But then, with a jet further penetration into a pool, due to instability of a jet causing by its free surface perturbations and by a loss of momentum, the jet area may change at any moment.

Strictly saying, this phenomenon revealed by simple integral analysis requires complete investigation of the instability with the bifurcation analysis, therefore it is a subject of a separate paper. Here only some estimation is been done for the moment.

3.5 Calculation of the examples to illustrate the results obtained

Starting penetration into a pool from S_1=1 the jet should become to a cross-section value S_1=2 at the point

$$h_1=\frac{Fr}{8(1-\rho_{21})}=\frac{1}{8Ri}\ ,$$

when further existence of the two possible jet's radiuses is impossible. Here $Ri=(1-\rho_{21})/Fr$ is the Richardson number (the ratio between the momentum and the buoyancy forces of a jet).

The phenomenon of a jet penetration into a pool of other liquid accounting the results obtained and the experimental data presented above may be explained as follows. The jet penetrates into a pool at the distance $h=h_0$ determined by the initial

length of a jet, the Froude number and the density ratio. In case of a long jet as well as the jet permanently spreading out of the nozzle the initial penetration length is determined by the Froude number and the density ratio. Then jet is going with an increase of its radius till $h = h_1$, which represents the bifurcation point. After this bifurcation point, the jet is abruptly switched and further goes with a nearly constant radius. Applying the solution obtained to those parts
with their own initial data, the whole jet might be computed based on the analytical solution obtained.

From the equation (13) a jet cross-section at the depth of penetration

$$h = h_0$$

is as follows:

$$S_1 = 0.5\rho_{12}(1 \pm \sqrt{1-4\rho_{21}})$$

where from for the density ratio 0.1 yield the following two available stable states of the jet:

$$S_1 \approx 1{,}15\,,\ r_1 \approx 1{,}07\,,\ v_1 \approx 0{,}87\,,$$

and

$$S_1 \approx 8{,}87\,,\ r_1 \approx 2{,}98\,,\ v_1 \approx 0{,}11\,,$$

where from one could see the approximate correspondence to the above experimental pictures.

4 The non-linear non-isothermal model of a jet penetration into the liquid pool of other density

4.1 Jet penetration into another liquid at the boiling and non-isothermal conditions

In many practical applications, for example during severe accidents at the nuclear power plants (NPP) the high-temperature corium melt jet is penetrating the pool of volatile coolant.

Then jet penetration into the coolant is going under the non-isothermal conditions and by action of the vapor flow against the jet. The schematic model for such case is presented in Fig.4. This model is taking into account the vapor pressure acting on the jet due to high temperature of the jet.

The other assumptions are similar to the previous model. The jet velocity is computed as $V_1 = dx/dt$, где x is coordinate from the pool surface into the pool by jet penetration, x=0 is the equation of the pool free surface at the rest. The jet radius is a, the length is h, then the initial jet velocity is V_0.

4.2 Mathematical model of the jet penetrating pool of volatile coolant

Development of the model for the described system is based on the momentum conservation equation written in the following form:

$$\rho_1 h \frac{dV_1}{dt} = g(\rho_1 h - \rho_2 x) - \alpha\rho_2 V_1^2 - \beta\rho R T_1\,, \quad (14)$$

where the cross-sectional area multiplayer $S_1=\pi a^2$ is omitted. Here g acceleration due to gravity, h is the cylindrical jet length, ρ is the density of the vapor, T_1 is the temperature of the vapor, R- universal gas constant, α- drag force coefficient (depends on the jet form and flow regime.

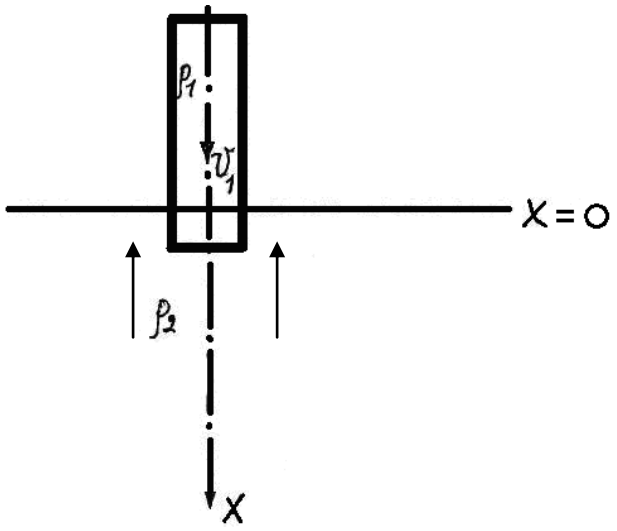

Fig.5. Schematic representation of the jet penetrating the pool of volatile coolant

We take the maximum value α=0.5 for conservative estimations, β- empirical constant to be computed from the experimental data (max β=1).

4.3 The Cauchy problem for the equation of the jet penetration

The non-linear differential equation (14) with the initial conditions:

$$t=0,\ \ x=0,\ \ \frac{dx}{dt} = V_n\,, \quad (15)$$

where $V_n=V_0$ for the thin jet and for the thick slow jets (or in a pool of small density), represent the Cauchy problem for this case.

The equation (15) is rewritten in the following form:

$$\frac{d^2x}{dt^2}+\alpha A(\frac{dx}{dt})^2+gAx+C=0\,, \qquad (16)$$

where $A=\rho_{12}/h$, $C=b/h-g$, with the $x\geq h$ the $Ax=\rho_{12}=const$.

The time t as a variable is present in the equation (16) implicitly, therefore the equation is autonomous. By $x\geq h$ the equation (16 transforms to

$$\frac{d^2x}{dt^2}+\alpha A(\frac{dx}{dt})^2+g\rho_{12}+C=0\,, \qquad (17)$$

4.4 Analytical solution of the equation array

The second-order non-linear differential equation (17) has analytical solution. For this, the equation better to transform to the dimensionless form, which is preferable in many cases as the most general one.

Thus, the Cauchy problem (17), (15) is transformed to a dimensionless form with the characteristic velocity V_0, characteristic distance a, and time a/V_0. Then dimensionless form of the above equation is getting the next form:

$$\frac{d\bar{x}}{dt}=\bar{v}\,,$$
$$\frac{d\bar{v}}{d\bar{t}}=-\left[\varepsilon\alpha\rho_{21}\bar{v}^2+\frac{1}{\mathrm{Fr}^2}(x\varepsilon\rho_{21}+\bar{b}-1)\right], \qquad (18)$$
$$\bar{x}\leq 1/\varepsilon\,;$$

$$\bar{t}=0\,,\quad \bar{x}=0,\quad \bar{v}=\bar{v}_n\,, \qquad (19)$$

where the last term in a second equation (18) by $\bar{x}>1/\varepsilon$ is equal to $(\rho_{21}\text{-}1)/\mathrm{Fr}^2$, $\mathrm{Fr}^2=V_0^2/(ga)$ – the Froude number, $\varepsilon=a/h$- the ration of the radius and the length of the round jet, $\bar{b}=n/V_0^2$- ratio of the vapor potential energy and kinetic energy of the jet, $\bar{v}_n=1$, or $\bar{v}_n=1-4\varepsilon\rho_{21}/(3\pi)$ if the shock of the jet and free surface of the rest pool is accounted.

General view of the autonomous equation array (18) has the next form

$$\frac{dx}{dt}=V\,,$$
$$\frac{dV}{dt}=-(\alpha AV^2+gAx+C)\,, \qquad (20)$$

where from follows that velocity of the penetrating jet tends to falling with time, except the case $Ax<1$, or $x<h\rho_{12}$, which corresponds to the initial stage of the jet penetration when

$$\alpha AV^2+g(Ax-1)+b/h<0\,,$$

or

$$V^2<gh(1-\rho_{21})-b\,,\ \text{by } x\geq h;$$

and

$$V^2>gh(1-\rho_{21})-b\,,\ \text{by } x<h,$$

where from seen that by substantially big influence of the vapor flow on a jet penetration this case is impossible, because otherwise it requires:

$$gh(1-\rho_{21})>b\,,\ \text{by } x\geq h$$

or

$$g(h-\rho_{21}x)>b\,,\ \text{by } x<h.$$

The mathematical model thus developed is applied for simulation of the corium jet penetrating the pool of volatile coolant under reactor vessel at NPP in the passive protection systems against severe accidents at NPP. For this, the dimensionless form (18), (19) and dimension forms (20) or (15)-(17) are applied.

4.5 Dimensionless analytical solution

With account of the above-mentioned, the analytical solution for the equation array (18) is got as follows:

$$\bar{x}=\frac{1}{\alpha\rho_{21}\varepsilon}\ln\left|\cos\left[\frac{1}{Fr}\sqrt{\frac{\rho_{21}-1+\bar{b}}{\alpha\rho_{21}\varepsilon}}(\bar{c}_1+\right.\right.$$
$$\left.\left.-\alpha\rho_{21}\varepsilon\bar{t}\,)\right]\right|+\bar{d}_1, \qquad (21)$$
$$\bar{V}=\frac{1}{Fr}\sqrt{\frac{\rho_{21}-1+\bar{b}}{\alpha\rho_{21}\varepsilon}}tg\left[\frac{1}{Fr}\sqrt{\frac{\rho_{21}-1+\bar{b}}{\alpha\rho_{21}\varepsilon}}(\bar{c}_1+\right.$$
$$\left.-\alpha\rho_{21}\varepsilon\bar{t}\,)\right],$$
$$\rho_{21}>1-\bar{b}\,;$$

$$\bar{x} = \frac{1}{\alpha\rho_{21}\varepsilon}\ln\left|\exp\left[\frac{1}{Fr}\sqrt{\frac{1-\rho_{21}-\bar{b}}{\alpha\rho_{21}\varepsilon}}(\bar{c}_2 - \alpha\rho_{21}\varepsilon\bar{t})\right] + \right.$$
$$\left. - \exp\left[\frac{1}{Fr}\sqrt{\frac{1-\rho_{21}-\bar{b}}{\alpha\rho_{21}\varepsilon}}(\alpha\rho_{21}\varepsilon\bar{t} - \bar{c}_2)\right]\right| + \bar{d}_2,$$

(22)

$$\bar{V} = -\frac{1}{Fr}\sqrt{\frac{1-\rho_{21}-\bar{b}}{\alpha\rho_{21}\varepsilon}} *$$
$$*cth\left[\frac{1}{Fr}\sqrt{\frac{1-\rho_{21}-\bar{b}}{\alpha\rho_{21}\varepsilon}}(\bar{c}_2 - \alpha\rho_{21}\varepsilon\bar{t})\right],$$
$$\rho_{21} < 1-\bar{b}, \quad \bar{V} > \frac{1}{F_r}\sqrt{\frac{1-\rho_{21}-\bar{b}}{\alpha\rho_{21}\varepsilon}};$$

$$\bar{x} = -\frac{1}{\alpha\rho_{21}\varepsilon}\ln\left|\exp\left[\frac{1}{Fr}\sqrt{\frac{1-\rho_{21}-\bar{b}}{\alpha\rho_{21}\varepsilon}}(\bar{c}_3 + \alpha\rho_{21}\varepsilon\bar{t})\right] + \right.$$
$$\left. + \exp\left[-\frac{1}{Fr}\sqrt{\frac{1-\rho_{21}-\bar{b}}{\alpha\rho_{21}\varepsilon}}(\bar{c}_3 + \alpha\rho_{21}\varepsilon\bar{t})\right]\right| + \bar{d}_3,$$

(23)

$$\bar{V} = -\frac{1}{Fr}\sqrt{\frac{1-\rho_{21}-\bar{b}}{\alpha\rho_{21}\varepsilon}}th\left[\frac{1}{Fr}\sqrt{\frac{1-\rho_{21}-\bar{b}}{\alpha\rho_{21}\varepsilon}}(\bar{c}_3 + \right.$$
$$\left. + \alpha\rho_{21}\varepsilon\bar{t})\right],$$
$$\rho_{21} < 1-\bar{b}, \quad \bar{V} < \frac{1}{Fr}\sqrt{\frac{1-\rho_{21}-\bar{b}}{\alpha\rho_{21}\varepsilon}}.$$

Here are: $\bar{c}_{1-3}, \bar{d}_{1-3}$ - constants to be computed from the initial conditions (19), $\bar{b} = b/(hg)$.

5 Study of the non-linear non-isothermal model of a jet penetration into the liquid pool of other density

5.1 Peculiar point of the equation array

The equation array (18) has peculiar point

$$\bar{x}_0 = (1-\bar{b})\rho_{12}/\varepsilon, \ \bar{v}_0 = 0,$$

which is for the jet without vaporization:

$$\bar{x}_0 = \rho_{12}/\varepsilon, \ \bar{v}_0 = 0.$$

But as far as (18) satisfies at the interval $\bar{x} \le 1/\varepsilon$, the peculiar point belongs to the determination region: $\rho_{21} \ge 1-\bar{b}$, what corresponds to the solution (21) after point $\bar{x} = 1/\varepsilon$.

If $\rho_{21} < 1-\bar{b}$, then a peculiar point is absent and solution after the point $x = 1/\varepsilon$ has the form (21) or (22) depending on the velocity of a jet penetration into a pool. A jet moves until the point $\bar{x} = 1/\varepsilon$ without any peculiarities and continues its movement after the point $\bar{x} = 1/\varepsilon$ in accordance with the solution (21)-(23) thus obtained.

In a peculiar point $\bar{x} = x_0$ the jet velocity becomes zero (jet stops – does not exist anymore as a jet or continues its movement if it is denser jet than a pool, due to gravitation).

The maximal penetration length of a jet into a pool by m<0 (jet velocity decreases with $\bar{x}$) is the same as by m>0 (jet velocity increases with $\bar{x}$). The difference is only that in a first case $\bar{V}_* > 0$ (jet is moving in a pool downwards), while in a second case $\bar{V}_* < 0$ (jet moves in the opposite direction – vertically up in a pool). Thus, a jet decelerates until the point of a rest and then moves up, or it stops at the point $\bar{x} = \bar{x}_*$ ($\bar{V}_* = 0$, by $m = 0$).

In an absence of vaporization in a pool ($\bar{b} = 0$), the peculiar point is absent if pool is lighter than a jet (or penetrating a pool solid body). The peculiar point is moving inside the pool (the jet penetration length is growing) with decrease of a jet radius and density ration of the pool and jet.

Vaporization in a pool decreases this critical level up to zero value, and available even shock due to a vapor explosion, $\bar{b} > 1$.

5.2 Phase trajectories of a jet

The second equation of the equation array (18) may be divided by the first one and get the following equation for the phase trajectories of the system:

$$\frac{d\bar{v}}{d\bar{x}} = -\frac{\varepsilon\alpha\rho_{21}Fr^2\bar{v}^2 + \varepsilon\rho_{21}\bar{x} + \bar{b} - 1}{Fr^2\bar{v}}, \qquad (24)$$

with the boundary conditions:

$$\bar{x}=0, \quad \bar{v}=\bar{v}_n. \tag{25}$$

The first-order differential equation (24) determines for each point $(\bar{x},\bar{v})$ the corresponding direction of the going through it curve $d\bar{v}/d\bar{x}$. Thus, a field of such directions («portrait» of the differential equation on a phase plane) allows producing a sketch $\bar{v}(\bar{x})$ and then determine the solution of the equation by the stated initial values of the $\bar{x}$ and $\bar{v}$. Let us start from the points of constant jet velocity directions $d\bar{v}/d\bar{x}=m$ (isoclines, or the lines of the equal jet velocity gradients).

According to the above stated:

$$\varepsilon\alpha\rho_{21}Fr^2\bar{v}^2+mFr^2\bar{v}+\bar{b}+\varepsilon\rho_{21}\bar{x}-1=0,$$

where from

$$\bar{v}_{1.2}=\frac{-mFr\pm\sqrt{m^2Fr^2-4\varepsilon\alpha\rho_{21}(\bar{b}+\varepsilon\rho_{21}\bar{x}-1)}}{2\varepsilon\alpha\rho_{21}Fr}. \tag{26}$$

Following the (26), one can get the condition for real jet velocity (real $\bar{v}$):

$$\bar{x}\le\bar{x}_*=\frac{\rho_{12}}{\varepsilon}\left(1+\frac{m^2Fr^2}{4\alpha\varepsilon}\rho_{12}-\bar{b}\right)=\bar{x}_0+\frac{m^2Fr^2}{4\alpha\varepsilon^2}\rho_{12}^2. \tag{27}$$

The equation (27) forecasts the maximal available length of a jet penetration into a pool by all possible parameters of the system of study. By m=0 for example (zero gradient, jet is moving with constant speed by $\bar{x}$) yields $\bar{x}_*=\bar{x}_0$.

The phase trajectories of a jet are illustrated in Fig. 6. There are available the following situations:

- $\rho_{21}\ge 1-\bar{b}$, the peculiar point is inside the definition region of the equations (18), $\bar{x}_0<1/\varepsilon$, and a jet can rich maximal penetration length ($\bar{x}_*\le 1/\varepsilon$) or continue its movement inside the pool according to the equations (21)-(23), if $\bar{x}_*>1/\varepsilon$;
- $\rho_{21}<1-\bar{b}$, the peculiar point is outside the definition region of the equations (18) ($\bar{x}_0>1/\varepsilon$, and by $\bar{x}_*>1/\varepsilon$ even stronger than previous condition), therefore a jet moves until the point $\bar{x}=1/\varepsilon$ without any peculiarities and continues movement after the point $\bar{x}=1/\varepsilon$ according to the equations (21)-(23).

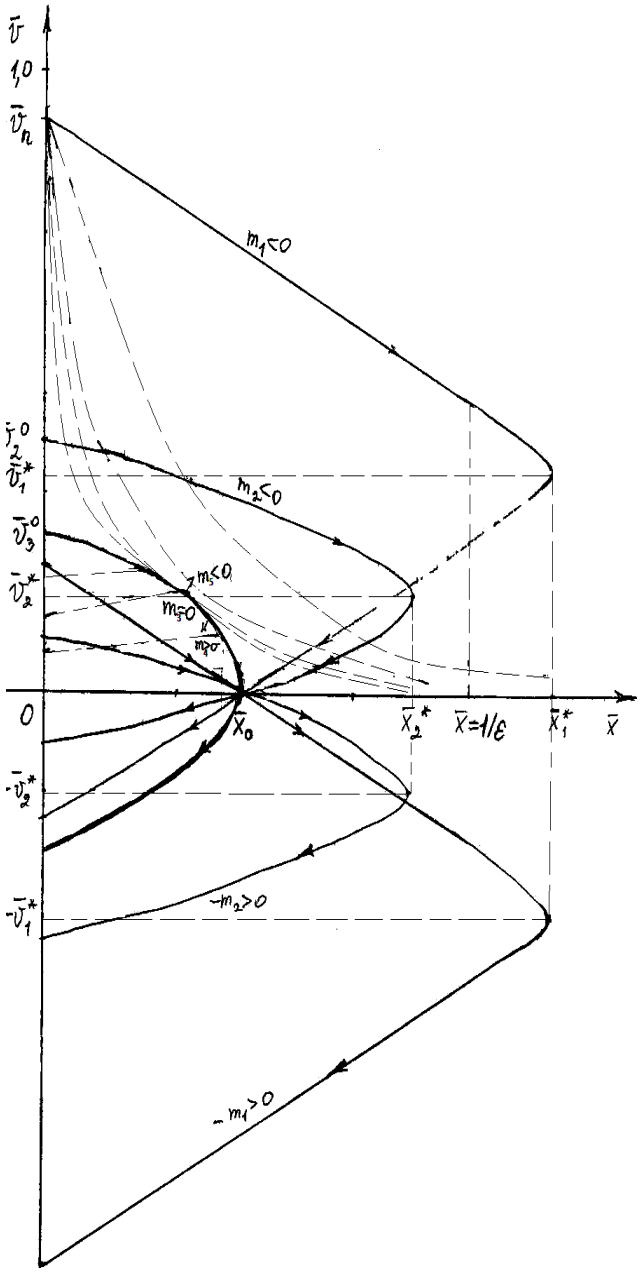

Fig.6. Phase portrait of a jet penetrating pool of volatile coolant

In a peculiar point $\bar{x} = x_0$ jet velocity equal zero and it stops.

5.3 Vapor explosion in a pool

In case of a vapor explosion in a pool (big difference in a temperature between a jet and a pool determines the process together a heat capacity factor) the jet penetration length may be short. One can estimate it by the initial maximal velocity gradient when a jet just starts to penetrate the pool:

$$m_0 = -\frac{\alpha\varepsilon\rho_{21}\bar{V}_n^2 Fr^2 + \bar{b} - 1}{Fr^2 \bar{V}_n}, \qquad (28)$$

Then by $\bar{b}_* = 1 + \alpha\varepsilon\rho_{21}\bar{V}_n^2 Fr^2$ a jet cannot penetrate a pool at all and with account of a shock on pool surface yields:

$$\bar{b}_* = 1 + \alpha\varepsilon\rho_{21} Fr^2 (1 - \frac{4\varepsilon}{3\pi}\rho_{21})^2, \qquad (29)$$

For a thin jet and low density of a pool (more generally, $\varepsilon\rho_{21} << 1$) the equation (29) results in $\bar{b}_* = 1 + \alpha\varepsilon\rho_{21} Fr^2$, which means by low jet velocity when $Fr^2 \sim 1$ or $Fr^2 << 1$ that a jet weight is equalized by the vapour pressure. By $Fr^2 >> 1$ the value of $\bar{b}_*$ may substantially prevail unite.

5.4 Numerical simulation of the system on computer

Some results of a computer simulations for the phase trajectories of a jet penetration into a pool of volatile coolant by the mathematical model developed were presented in Fig.6.

Let us analyze the results more in deep. The phase trajectories were presented for the next conditions:

$$m_1 = (\frac{d\bar{V}}{d\bar{x}})_{\bar{x}=0} < 0, \quad m_2 < 0, \quad m_2 > m_1,$$
$$m_3 = 0, \quad m_4 > 0, \quad m_4 = -m_2,$$
$$m_5 > 0, \quad m_5 = -m_1,$$

$\bar{x}^*$ is a maximal jet penetration into a pool and x_0 is a such critical point that all the trajectories (all isoclines) are going through it up to a point of the jet rest.

A peculiarity of the results obtained, as shown in Fig.6, is symmetry of the phase portrait with regards to an axis *x* for the same values of the parameter *m* of the opposite signs. The trajectory for *m*=0 is symmetrical regarding the axis *x*. Dashed lines depict trajectories of a jet for different available conditions of its penetration into a pool. An interesting peculiarity is that none of the jet trajectories goes through the phase trajectory *m*=0, independently of the starting jet penetration velocity (initial jet velocity gradient *m*).

5.5 Specific features of the results obtained

Despite a remarkable number of the papers done on a subject [20-31], the results obtained revealed some special features of a jet penetration into a pool, which may be of interest for the experts, both theoretical and experimental one.

6 Conclusion

The jet penetrating a pool of other liquid was investigated for different conditions. The problem is of interest for modelling and simulation of the severe NPP accidents in touch with development and operation of the passive protection systems. Analyses on the penetration phenomena of a jet into another liquid at the isothermal and non-isothermal conditions were performed and compared to the data from literature. The non-linear analytical models for the jet to predict the maximum penetration into a pool were developed and reasonably described the characteristics of the penetration behaviours.

The results of the mathematical modelling and simulation of the jets penetrating the pool of other liquid under diverse conditions as well as an analysis of the experimental data have clearly shown that the falling buoyant jets penetrating the pool of other liquid are quite different from the classical jets going under pressure gradient. For example, the classic scheme with monotone jet radius evolution does not work in this case. There is clearly observed phenomenon that jet is going with nearly constant radius up to some point in a pool, then at the point of "bifurcation" it substantially changes its radius abruptly (jet switches its one constant radius to the other one). These specific peculiarities of the penetrating jets were discussed and explained.

References:

[1] R.J. Eichelberger, Experimental test of the theory of penetration by metallic jets, Journal

of Applied Physics, Vol.27, No.1, 1956, pp. 63-68.

[2] M.I. Gurevich, Theory of jets in ideal fluids, Translated from the russian edition by: Robert l. Street and Konstantin Zagustin, Academic press, New York/London, 1965.

[3] J.S. Turner, Jets and plumes with negative or reversing buoyancy, Journal of Fluid Mechanics, Vol.26, No.4, 1966, pp. 779-792.

[4] M.A. Lavrent'ev and B.V. Shabat, The problems of hydrodynamics and their mathematical models, Moscow, Nauka, 1973 (In Russian).

[5] J. Carleone, R. Jameson and P. C. Chou, The tip origin of a shaped charge jet, Propellants and Explosives, Vol.2, No.6, 1977, pp. 126-130.

[6] E. Hirsch, A formula for the shaped charge jet breakup-time, Propellants and Explosives, Vol.4, No.5, 1979, pp. 89-94.

[7] M.L. Corradini, B.J. Kim, M.D. Oh, Vapor explosions in light water reactors: A review of theory and modeling, Progress in Nuclear Energy, Vol.22, No.1, 1988, pp. 1-117.

[8] M. Saito, et al. Experimental study on penetration behaviors of water jet into Freon-11 and Liquid Nitrogen, ANS Proceedings, Natl. Heat Transfer Conference, Houston, Texas, USA, July 24-27, 1988.

[9] R.W. Cresswell, R.T. Szczepura, Experimental investigation into a turbulent jet with negative buoyancy, Physics of Fluids, A5, No.11, 1993, pp. 86-107.

[10] M. Epstein, H.K. Fauske, Steam film instability and the mixing of core-melt jets and water. ANS proceedings. National heat transfer conference. Aug. 4-7. Denver, Colorado, 1985.

[11] D. F. Fletcher, The particle distribution of solid melt debris from molten fuel-coolant interaction experiments. Nuclear Engineering and Design, No.105, 1988.

[12] D.F. Fletcher, A. Thyagaraja, The CHYMES mixing model, Progress in Nuclear Energy, Vol.26, No.1, 1991, pp. 3161.

[13] S.A. Kinelovsky and K.K. Maevsky, On the cumulative jet penetration into hard plate, Journal of Applied Mathematics and Technical Physics, No.2, 1989, pp. 97-105 (In Russian).

[14] A.L. Yarin, Free liquid jets and films: hydrodynamics and rheology, Longman Scientific & Technical, Haifa, 1993.

[15] D. Goldman, Y. Jaluria, Effect of opposing buoyancy on the flow in free and wall jets, Journal of Fluid Mechanics, Vol.166, 1986, pp. 41-56.

[16] H.O. Haraldsson, I.V. Kazachkov, T.N. Dinh and B.R. Sehgal, Analysis of thin jet breakup depth in immiscible fluids, Abstracts of the 3rd International Conference on Advances in Fluid Mechanics, 24-26 May Montreal, Canada, 2000.

[17] H.S. Park, I.V. Kazachkov, B.R. Sehgal, Y. Maruyama and J. Sugimoto, Analysis of Plunging Jet Penetration into Liquid Pool in Isothermal Conditions, ICMF 2001: Fourth International Conference on Multiphase Flow, New Orleans, Louisiana, U.S.A., May 27 - June 1, 2001.

[18] G.N. Abramovich, L. Schindel, The Theory of Turbulent Jets, MIT Press, 1963.

[19] I.V.Kazachkov, D.Paladino and B.R. Sehgal, Ex-vessel coolability of a molten pool by coolant injection from submerged nozzles/ 9th Int. Conf. Nucl. Energy Devel. Nice, France, April 8-12, 2001.

[20] F. Bonetto, D. Drew and R.T. Lahey, Jr., The analysis of a plunging liquid jet-air entrainment process, Chemical Engineering Communications, Vol.130, 1994, pp. 11-29.

[21] A.M. Lezzi, A. Prosperetti, The stability of an air film in a liquid flow, Journal Fluid Mechanics, Vol.226, 1991, pp. 319-347.

[22] P. Lara, Onset air entrainment for a water jet impinging vertically on a water surface, Chemical Engineering Sciences, Vol.34, 1979, pp. 1164-1165.

[23] G.K. Batchelor, An Introduction to Fluid Dynamics, New York: Cambridge University Press, 1967.

[24] P.L. Sachdev, Non-linear ordinary differential equations and their applications, Marcel Dekker, Inc., 1991.

[25] J. Dahlsveen, R. Kristoffersen and L. Saetran, Jet mixing of cryogen and water. In Turbulence and Shear Flow Phenomena, 2nd International Symposium (Lindborg, Johansson, Eaton, Humphrey, Kasagi, Leschziner and Sommerfeld, eds.), KTH Stockholm, Sweden, June 27-29, 2, 2001.

[26] I.V. Kazachkov, A.H. Moghaddam, Modeling of thermal hydraulic processes during severe accidents at nuclear power plants, National Technical University of Ukraine “KPI”, Kyiv, 2008 (in Russian).

[27] Lin, S.P. and Reitz, R.D., Drop and spray formation from a liquid jet, Annual Review of Fluid Mechanics, Vol. 30, 1998, pp. 85-105.

[28] W.C. Yang and D.L. Keairns, in Fluidization, D.L. Keairns and J.F. Davidson (eds.), Cambridge Univ. Press, Cambridge, 1978.

[29] T.R. Blake, H. Webb and P.B. Sunderland, The Nondimensionalization of Equations Describing Fluidization with Application to the Correlation of Jet Penetration Height, Chemical Engineering Society, Vol.45, No.2, 1990, pp. 365-371.

[30] C.Z. Weber, Zum Zerfall eines Fluessigkeitsstrahles, Zeitschrift fuer Angewandte Mathematik und Mechanik, Vol.11, 1931, pp. 136-154.

[31] V.M. Entov and A.L. Yarin, The dynamics of thin liquid jets in air, Journal of Fluid Mechanics, Vol.140, 1984, pp. 91-111.